

# Simulation of Copolymer Bottle-Brushes

Hsiao-Ping Hsu,\* Wolfgang Paul, Kurt Binder

**Summary:** The structure of bottle-brush polymers with a rigid backbone and flexible side chains is studied in three dimensions, varying the grafting density, the side chain length, and the solvent quality. Some preliminary results of theoretical scaling considerations for one-component bottle-brush polymers in a good solvent are compared with Monte Carlo simulations of a simple lattice model. For the simulations a variant of the pruned-enriched Rosenbluth method (PERM) allowing for simultaneous growth of all side chains in the Monte Carlo sampling is employed. For a symmetrical binary (A,B) bottle-brush polymer, where two types (A,B) of flexible side chains are grafted with one chain end to the backbone in an alternating way, varying repulsive binary interactions between unlike monomers and the solvent quality, it is found that phase separation into an A-rich part of the cylindrical molecule and a B-rich part can occur only locally. Long range order (in the direction of the backbone) does not occur, and hence the transition from the randomly mixed state of the bottle-brush to the phase-separated structure is strongly rounded, in contrast to the corresponding mean field predictions of a sharp transition to a “Janus cylinder” phase-separated structure. This lack of a phase transition can be understood from an analogy with spin models in one dimension. By estimating the correlation length for this phase separation along the backbone as a function of side chain length and solvent quality, we present strong evidence that no sharp phase transition occurs.

**Keywords:** conformational analysis; copolymerization; macromolecules; Monte Carlo simulation; phase separation

## Introduction

Bottle-brush polymers are macromolecules with a comb-like architecture, where flexible side chains are densely grafted to a linear long macromolecule which forms the backbone chain. If the backbone is a rigid polymer, its solubility and processability are improved.<sup>[1–3]</sup> If the grafting density of the side chains is very high, it is in the form of a rather stiff cylindrical “bottle brush”-shaped object, which under certain conditions shows a thermally induced collapse transition to a spherical structure, providing interesting perspectives for the design of “molecular actuators”.<sup>[4]</sup> In the present work, we focus on the following two

problems: (i) the conformation of a side chain of one-component bottle-brush polymers, where the backbone is treated as a rigid straight line or thin cylinder,<sup>[5–6]</sup> and (ii) the phase separation of copolymer bottle-brushes with a rigid backbone, where two types (A,B) of flexible side chains are grafted with one chain end to the backbone in an alternating way. In problem (i), the stretching of the side chains in the radial direction in the case of sufficiently high grafting density was mostly discussed in terms of a scaling description,<sup>[5–9,13–15]</sup> extending the Daoud-Cotton<sup>[17]</sup> “blob picture”<sup>[18–20]</sup> from star polymers to bottle-brush polymers. If one uses the Flory exponent<sup>[21,22]</sup>  $\nu = 3/5$  in the scaling relation for the average root mean square end-to-end distance of a side chain in a radial direction,  $R_{e-e} \propto \sigma^{(1-\nu)/(1+\nu)} N^{2\nu/(1+\nu)}$ , where  $\sigma$  is the grafting density and  $N$  is the number

Institut für Physik, Johannes Gutenberg-Universität Mainz, D-55099 Mainz, Staudinger Weg 7, Germany  
E-mail: hsu@uni-mainz.de

of effective monomeric units of a side chain, one obtains  $R_{e-e} \propto \sigma^{1/4} N^{3/4}$ . The resulting exponents happen to be the same as for quasi-two-dimensional configurations of a chain one would obtain by assuming each chain is confined to a disk of width  $\sigma^{-1}$ .<sup>[16]</sup> Although this latter picture is a misconception, in experimental studies [e.g. Ref.<sup>[23,24]</sup>] this hypothesis of quasi-two-dimensional chains is discussed as a serious possibility. Therefore we find that it is necessary to give a detailed discussion of the scaling concepts based on the blob picture for bottle-brush polymers with rigid backbone and verify the theoretical prediction by computer simulations with the pruned-enriched Rosenbluth method (PERM).<sup>[25–27]</sup>

Concerning the second problem, recently the existence of a local phase separation along the backbone of the bottle-brush giving rise to “horseshoe” and “meander”-like structures of copolymer bottle-brushes was observed in experiments.<sup>[28]</sup> The problem of phase separation within a simple copolymer bottle-brush has also drawn attention both by analytical theory<sup>[29]</sup> and computer simulation.<sup>[30,31]</sup> In Ref.,<sup>[29,30]</sup> authors gave the predictions of how the phase transition point from the randomly mixed state (where both *A* and *B* monomers are homogeneously distributed in the cylinder volume) to the separated state depends on the chain length *N* of the side chains and also suggested the possibility to create “Janus cylinders” (upper half of the cylinder containing the *A* monomers, lower half containing the *B* monomers). Recently, Hsu et. al.<sup>[31]</sup> reconsidered this problem noting that for any finite chain length *N* also the cylinder radius (or brush “height”) *h* is finite, and hence the system is quasi-one-dimensional. In one-dimensional systems with short range interactions at nonzero temperatures no long range order is possible. Thus this problem can be related to the one-dimensional XY-model. The Flory-Huggins parameter  $\chi_{AB}$  that describes the incompatibility between *A* and *B* monomers takes the role that  $J/k_B T$  plays for the spin model. However, the problem whether for  $N \rightarrow \infty$  (and depend-

ing on the solvent condition) sharp phase transitions are restored is nontrivial, and in particular, describing the extent of rounding of the (mean field) transitions described in<sup>[29]</sup> by these long range fluctuations along the chain backbone remains a challenge. Performing Monte Carlo simulations with PERM<sup>[25–27]</sup> of a similar model as in Ref.,<sup>[30]</sup> a detailed conformational analysis of copolymer bottle-brushes is described in the latter section.

## Model and Simulation Method

Here, we consider the simplest lattice model of polymers, namely, the self-avoiding walk on a simple cubic lattice. The backbone of a copolymer bottle-brush is treated as a completely rigid rod with length  $L_b$ , oriented along the *z*-axis of a simple cubic lattice. The grafting density  $\sigma$  is defined by  $\sigma = n_c/L_b$ , where  $n_c$  is the total number of side chains. The side chains are grafted to the backbone with equal distance  $\sigma^{-1}$  and the side chains of two types *A* and *B* (note that  $B=A$  for one-component bottle-brush polymers) are grafted regularly in an alternating way. In order to avoid any effects due to the ends of a finite backbone, periodic boundary conditions are introduced in the *z*-direction. Assuming that there is only excluded volume interaction between monomers on the backbone and monomers on the side chains, but there are nearest neighbor interactions  $\epsilon_{AB}$ ,  $\epsilon_{AA} = \epsilon_{BB} = \epsilon$  between the respective pairs of monomers, the partition sum for this model is

$$Z = \sum_{\text{walks}} q^{m_{AA}+m_{BB}} q_{AB}^{m_{AB}}, \quad (1)$$

where  $q = e^{-\epsilon/k_B T}$ ,  $q_{AB} = e^{-\epsilon_{AB}/k_B T}$ , and  $m_{AA}$ ,  $m_{BB}$ ,  $m_{AB}$  are the numbers of non-bonded nearest neighbor monomer pairs *AA*, *BB*, and *AB*, respectively. The sum in Equation (1) extends over all possible configurations of these walks. Varying  $q$  in the range  $1 < q < 1.5$ , we cover the full range from good solvents ( $q=1$ ) to poor solvents ( $q=1.5$ ), since the  $\theta$ -solvent

corresponds to a choice<sup>[25]</sup>  $q_\theta = e^{-\varepsilon/k_B T_\theta} \approx 1.3087$ . We vary  $q_{AB}$  in the range  $0 \leq q_{AB} \leq q$ : The case  $q_{AB} = 0$  corresponds to a very strong repulsion between A and B, while for  $q_{AB} = q$  the chemical incompatibility  $\chi_{AB}$  vanishes [recall that<sup>[22]</sup>  $\chi_{AB} \propto \varepsilon_{AB} - (\varepsilon_{AA} + \varepsilon_{BB})/2$ ].

For our simulations, we use the algorithm PERM<sup>[25]</sup> which is a biased chain growth algorithm with resampling (“population control”) and depth-first implementation. Polymer chains are built like random walks by adding one monomer at each step. As in any such algorithm there is a wide range of possible distributions of sampling, we have the freedom to give a bias at each step while the chain grows, and the bias is corrected by means of a weight given to each sample configuration. In order to limit the fluctuations in weight as the chain is growing, the population control is done by “pruning” configurations with too low weight and “enriching” the sample with copies of high-weight configurations. Similar to a recent study of star polymers,<sup>[26,27]</sup> the bottle-brush is generated by adding one monomer to each side chain until all side chains have the same number of monomers, thus growing all side chains simultaneously. For efficiency, side chains are grown with higher probabilities in the directions perpendicular to the backbone and in the direction where there are more free next neighbor sites. This additional bias must be taken into account by suitable weight factors.

## Theory and Numerical Results

### A. One-component Bottle-brush Polymers in a Good Solvent

In a blob picture, according to the cylindrical geometry of bottle-brush polymers with rigid backbone, the space is partitioned into blobs of non-uniform size and shape (Figure 1). The blobs are characterized by one effective radius  $\xi(r)$  depending on the radial distance  $r$  from the cylinder axis. One considers a segment (e.g. the  $i$ th row in Figure 1) of the array of length  $L$

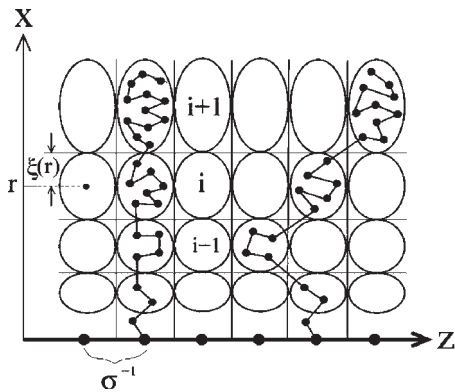


**Figure 1.** Schematic drawing of a blob picture for a bottle-brush polymer cut through the cylinder along the  $xz$ -plane containing the cylinder axis (backbone).

containing  $p$  polymer chains.<sup>[8]</sup> On a surface of a cylinder of radius  $r$  and length  $L$  there should then be  $p$  blobs, each of cross-sectional area  $\xi^2(r)$  (geometrical factors of order unity are ignored throughout). Since the surface area of the cylindrical segment is  $Lr$ , we must have<sup>[8,9,15]</sup>

$$p\xi^2(r) = Lr, \quad \xi(r) = (Lr/p)^{1/2} \\ = (r/\sigma)^{1/2}. \quad (2)$$

If the actual non-spherical shape of the blobs is neglected, the blob volume clearly is of the order of  $\xi^3(r) = (r/\sigma)^{3/2}$ . Using the principle that inside a blob self-avoiding walk statistics holds, we obtain

$$\xi(r) = a[n(r)]^\nu, \quad \text{and, } n(r) \\ = [\xi(r)/a]^{1/\nu} = [r/(a^2\sigma)]^{1/2\nu}, \quad (3)$$

here  $a$  is a length of the order of the size of an effective monomer, and  $n(r)$  is the number of monomers contained within a blob. The prediction of the power law decay for the density profile  $\rho(r)$  is therefore derived as follows<sup>[8,9,15,32]</sup>

$$\rho(r) = n(r)/\xi^3(r) \\ = a^{-3}[r/(a^2\sigma)]^{-(3\nu-1)/2\nu} \\ \approx a^{-3}[r/(a^2\sigma)]^{-0.65}, \quad \nu \approx 0.588. \quad (4)$$

Now the average height  $h$  of the bottle-brush is obtained by requiring that

integrating  $\rho(r)$  from  $r=0$  up to  $r=h$  all  $\sigma N$  monomers per unit length in  $z$ -direction are counted

$$\sigma N = \int_0^h \rho(r) r dr \propto a^{-3} (a^2 \sigma)^{(3\nu-1)/2\nu} \int_0^h r^{(1-\nu)/2\nu} dr, \quad (5)$$

and hence

$$N = (a\sigma)^{(v-1)/2\nu} (h/a)^{(v+1)/2\nu} \quad (6)$$

and

$$h = (a\sigma)^{(1-\nu)/(1+\nu)} N^{2\nu/(1+\nu)} = (a\sigma)^{0.259} N^{0.74}. \quad (7)$$

When  $\sigma \rightarrow 0$  one should expect a mushroom regime where there are no interactions between side chains. Side chains behave as self-avoiding walks in three dimensions, and the average height scales as  $h \propto N^\nu$ . We verify that this occurs for a lateral distance  $\sigma^{-1} \propto N^\nu$  between grafting points along the rigid backbone:

$$N^\nu \propto \sigma^{-(1-\nu)/(1+\nu)} N^{2\nu/(1+\nu)} \Rightarrow \sigma \propto N^{-\nu}. \quad (8)$$

This argument shows that  $\sigma^{-1}$  needs to be compared with  $N^\nu$ , so we can give a cross-over ansatz as follows,

$$h = N^\nu \tilde{h}(\eta = \sigma N^\nu), \quad (9)$$

where the scaling function  $\tilde{h}(\eta) \propto \eta^{(1-\nu)/(1+\nu)}$  for  $\eta \gg 1$ , and  $\tilde{h}(\eta) \approx \text{const}$  for  $\eta \rightarrow 0$ . As shown in Figure 1, the blobs are not circles but rather ellipses in the  $xz$ -plane, hence the 3D geometric shape of blobs are ellipsoids with three different axes,  $\sigma^{-1}$  in  $z$ -direction along the cylindrical axis,  $r$  is the  $y$ -direction (tangential on the cylinder surface, normal to  $z$ ), and the geometric mean of the two lengths,  $\sqrt{r\sigma^{-1}}$ , in the radial ( $x$ ) direction. Since the physical meaning of a blob is that of a volume region in which the excluded volume interaction is not screened, this result implies that the screening of excluded volume happens in a brush consisting of polymers grafted to a line in a very anisotropic way: actually there are three different screening lengths,  $\sigma^{-1}$  in the axial  $z$ -direction,  $\sqrt{r\sigma^{-1}}$  in the radial  $r$ -direction, and  $r$  in the third tangential  $y$ -direction. It is

still an open problem to verify that such a property of very anisotropic screening actually occurs. However, the volume of the ellipsoid with these three axes still reads

$$V_{\text{ellipsoid}} = (\sigma^{-1})(r)(r\sigma^{-1})^{1/2} = (r/\sigma)^{3/2} = \xi^3(r), \quad (10)$$

with  $\xi(r)$  given by Equation (3), hence the prediction of the density profile  $\rho(r)$ , Equation (4), and the average height  $h$ , Equation (7), are unchanged by the spherical approximation.

In order to verify the above theoretical prediction of the scaling behavior of side chains, we simulate one-component bottle-brush polymers in a good solvent, i.e.  $q=1$ , and  $q_{AB}=1$  in Equation (1), and choose backbone length  $L_b=32, 64$ , and 128, and grafting densities  $\sigma=1/32, 1/16, 1/8, 1/4, 1/2$ , and 1. The side chain length  $N$  was varied up to 2000. A snapshot of the configuration of a typical bottle-brush polymer with  $L_b=128$ ,  $\sigma=1/4$  (i.e.,  $n_c=32$  side chains) and side chain length  $N=2000$  containing a total number of monomers  $N_{\text{tot}}=L_b+n_c N=64128$  is shown in Figure 2. The average height of bottle-brush polymers is estimated by taking the average of the backbone-to-end distance perpendicular to the direction of backbone (along the  $z$ -axis) for all side chains, i.e.

$$R_h(N, \sigma) = \langle R_{b-e,x}^2(N, \sigma) + R_{b-e,y}^2(N, \sigma) \rangle^{1/2}. \quad (11)$$

According to the cross-over scaling ansatz, Equation (9), we plot  $R_h^2(N, \sigma)/N^{2\nu}$  against  $\eta = \sigma N^\nu$  for various values of backbone length  $L_b$  and grafting density  $\sigma$ , and take the value of  $\nu = \nu_3 \approx 0.58765$  given by the best estimate for 3d self-avoiding walks by PERM<sup>[25]</sup> in Figure 3. We see that systematic deviations from scaling occur for small  $L_b$ , large  $N$  and not too large  $\sigma$  in Figure 3a, which is due to artifacts created by periodic boundary conditions in our model. Each side chain interacts with its own periodic image in the region where its extension along the direction of backbone is larger than  $L_b/2$ . Removing these unphysical data, the nice

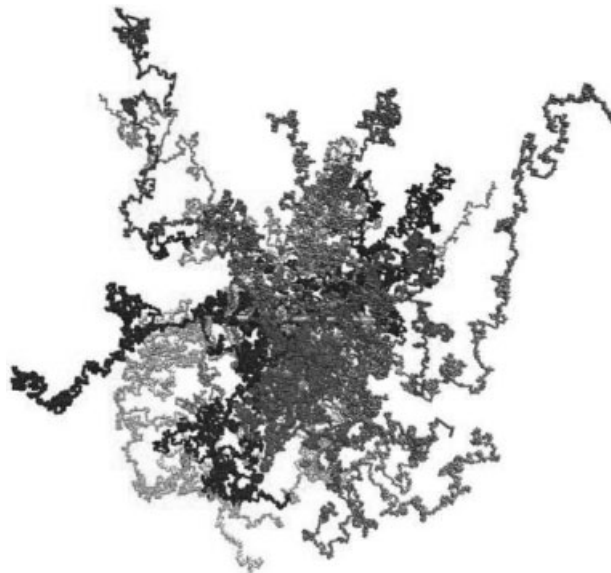


**Figure 2.**

Snapshot of a bottle-brush polymer with  $L_b = 128$ ,  $\sigma = 1/4$ , and  $N = 2000$  on the simple cubic lattice.

data collapse shown in Figure 3b results as predicted in Equation (9). As  $\eta$  increases, we see a cross-over from the mushroom behavior to the stretched bottle-brush polymers. Although only mild stretching of the side chains away from the backbone is obtained, which is still far away from the strong stretching predicted by scaling considerations, this cross-over behavior has not

been obtained by any other numerical simulations before.

### B. Copolymer Bottle-brushes

As mentioned in the introduction, the phase separation problem of copolymer bottle-brushes is like the one-dimensional

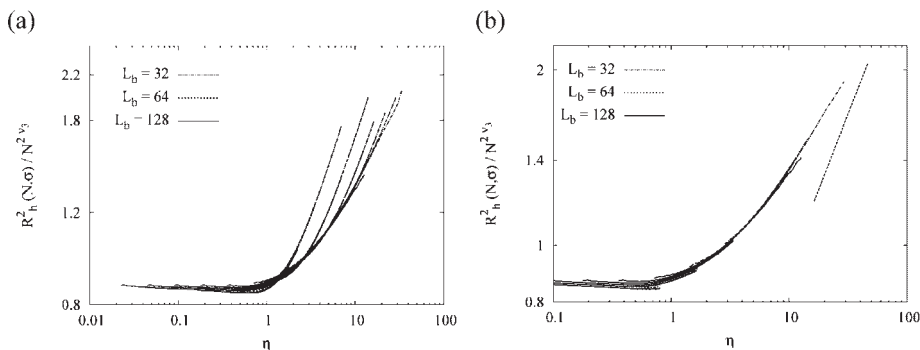


**Figure 3.**

Log-log plot of  $R_g^2(N, \sigma) / N^{2\nu_3}$  vs.  $\eta = \sigma N^{\nu_3}$ , with  $\nu_3 = 0.58765$  (a) including all data, and  $n_c = \sigma L_b = 1, 2, 4, 8, 16$ , and  $32$  from left to right for  $\eta < 1$ , (b) after removing all unphysical data due to periodic boundary conditions. The asymptotic behavior for  $\eta \gg 1$  is shown by the straight line with slope  $2(1 - \nu_3)(1 + \nu_3) \approx 0.519$  from Equation (9).

XY-model. In the XY-model, one considers a chain of spins on a one-dimensional lattice where each spin at site  $i$  is described by an angle  $\varphi_i$  in the  $xy$  plane, with  $0 \leq \varphi_i \leq 2\pi$ , and where neighboring spins are coupled. The coupling is described by the Hamiltonian

$$\begin{aligned}
 H &= -J \sum_i \cos(\varphi_{i+1} - \varphi_i) \\
 &= -J \sum_i \vec{S}_{i+1} \cdot \vec{S}_i,
 \end{aligned}
 \tag{12}$$

where  $\vec{S}_i = (\cos \varphi_i, \sin \varphi_i)$  is a unit vector in the  $xy$ -plane. While mean field theory predicts that ferromagnetic order (cf. Figure 4a) occurs along the chain for temperatures  $T < T_c^{MF} = cJ$ , where  $c$  is a constant of order unity,<sup>[33]</sup> an exact solution of this problem<sup>[33,34]</sup> shows that ferromagnetic long range order is unstable against long wavelength fluctuations, and actually the ferromagnetic correlation length  $\xi$  grows completely gradually as the temperature is lowered,

$$\xi = 2a(J/k_B T)
 \tag{13}$$

$a$  being the lattice spacing. Thus  $\xi$  has to diverge when  $T_c = 0$  is approached, and the singularity of  $\xi$  predicted by mean field theory at  $T = T_c^{MF}$  is completely washed out. This consideration can be generalized to cylinders of cross section area  $\pi R^2$ .<sup>[35]</sup> Equation (13) gets replaced by a more complicated behavior that is sketched in

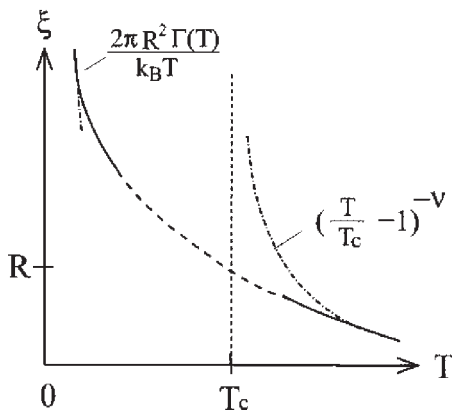


**Figure 5.** Crossover scaling behavior of the correlation length  $\xi$  as a function of temperature  $T$ .  $\xi \propto (T/T_c - 1)^{-\nu}$  for  $T > T_c$ , and  $\xi \propto R^2 \Gamma(T)/k_B T$  for  $T < T_c$ .  $T_c$  is the critical temperature of the corresponding bulk three-dimensional system.

Figure 5, but is still similar to Equation (13) at low temperatures

$$\begin{aligned}
 \xi &= 2\Gamma(T)\pi R^2/k_B T \\
 &\propto (R^2/a)(J/k_B T).
 \end{aligned}
 \tag{14}$$

Note that the “spinwave stiffness” (helicity modulus)  $\Gamma(T)$  characterizes the cost of long wavelength order parameter rotations, and  $\Gamma(T \rightarrow 0) \propto J$ . We suggest that the correlation length describing phase separation of a “Janus cylinder” type behaves qualitatively similar to Equations (13) and (14), cf. Figure 4b.<sup>[31]</sup>

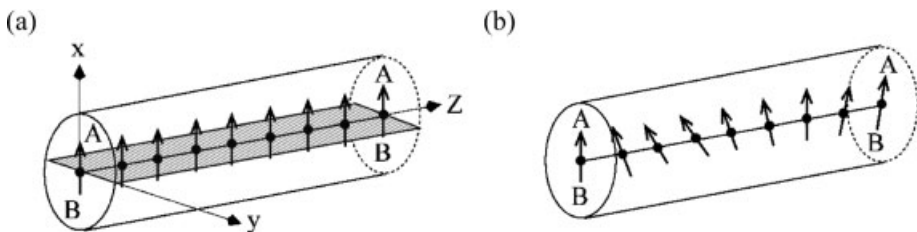


**Figure 4.** Schematic drawing of perfect phase separation of side chains in a binary (A,B) bottle-brush with alternating grafting sequence ABAB... into a “Janus cylinder” structure (a), where the A-chains occupy the upper part of the cylinder, and B-chains occupy the lower part of the cylinder. The orientation of the interface (a sharp shaded plane in the  $yz$ -plane) between them can be characterized by a vector oriented perpendicular to it (arrows). At nonzero but low temperature phase separation will occur locally, but entropy will lead to long-wavelength fluctuations of the orientation of this vector (b), destroying axial long range order along the direction of the backbone of the bottle brush.

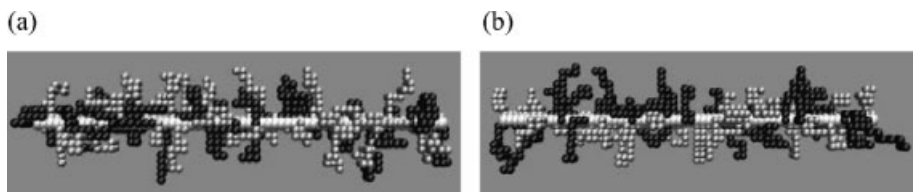


**Figure 6.**

Snapshots of the copolymer bottle brushes for a good solvent ( $q=1$ ),  $L_b=64$ ,  $N=18$ , (a)  $q_{AB}=1.0$  and (b)  $q_{AB}=0.1$ . Monomers A, monomers B, and monomers on the backbone are shown in black, gray and white colors, respectively.

We simulate binary bottle-brush polymers of backbone length  $L_b=32, 48$ , and  $64$ , in a good solvent ( $q=1$ ) and in a poor solvent ( $q=1.5$ ). Varying the parameter  $q_{AB}$  which controls the chemical incompatibility, typical snapshots of the conformations of bottle brush polymers for backbone length  $L_b=64$ , side chain length  $N=8$ , grafting density  $\sigma=1$ , are shown in Figures 6 and 7. In a poor solvent, side chains form more compact configurations (Figure 7), which is due to the fact that a very long single chain would experience a

collapse transition.<sup>[22]</sup> As  $q_{AB}$  becomes small, we see a more pronounced local phase separation along the backbone of the copolymer bottle-brush, although there still no long range order is present. In analogy to the spin model in one dimension, a simple way to define a unit vector  $\vec{S}_i^\alpha$  characterizing the orientation of the chain is that we draw a vector from each grafting site to the center of mass (CM),  $\vec{R}_{cm,i}^\alpha$ , of each side chain  $i$  of type  $\alpha$  ( $\alpha=A$  or  $B$ ), project this vector into the  $xy$ -plane, and normalize it (Figure 8). Since side chains of two types  $A$

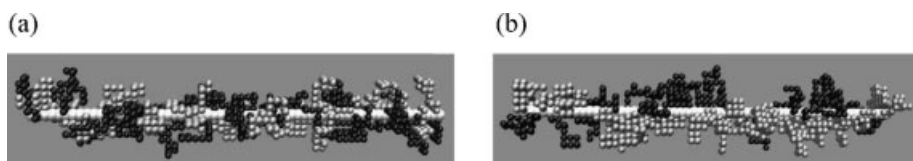


**Figure 7.**

Snapshots of the copolymer bottle brushes for a poor solvent ( $q=1.5$ ),  $L_b=64$ ,  $N=18$ , (a)  $q_{AB}=1.5$  (mixed state) and (b)  $q_{AB}=0.1$  (state with local phase separation). Monomers A, monomers B, and monomers on the backbone are shown in black, gray and white colors, respectively.

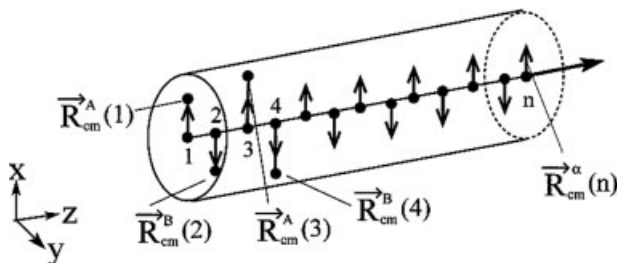


**Figure 8.**

Construction of vectors  $\vec{R}_{cm}^\alpha(n)$  from the grafting site  $n$  to the  $xy$ -component of the center of mass of the respective chain  $\alpha$ , and corresponding unit vectors (denoted by arrows). For a perfectly phase separated structure with the interface between A and B being the  $yz$ -plane, for  $\alpha=A$  all unit vectors point along the positive  $x$ -axis and for  $\alpha=B$  all unit vectors point along the negative  $x$ -axis.

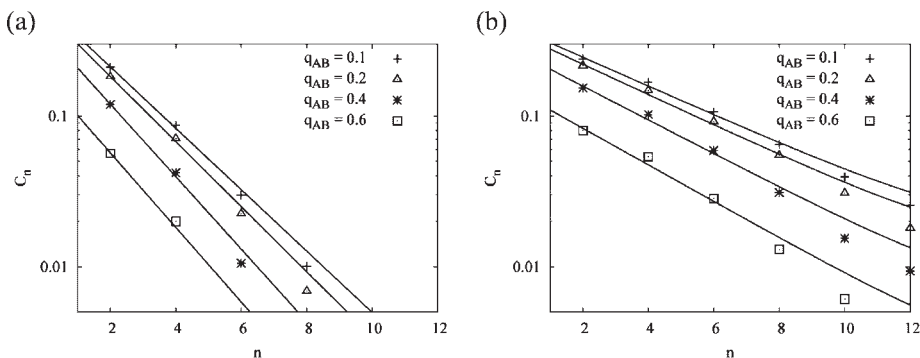


**Figure 9.**

Correlation function  $C_n$  plotted vs.  $n$  on a semi-log scale, for a good solvent ( $q=1.0$ ),  $L_b=32$ , (a)  $N=6$  and (b)  $N=18$ . Several choices of  $q_{AB}$  are included, as indicated.

and  $B$  are grafted to the backbone in an alternating way, i.e.  $ABAB\dots$ , we define a correlation function  $C_n$  as follows

$$C_n \equiv \left[ \langle \vec{S}_i^A \cdot \vec{S}_{i+n}^A \rangle + \langle \vec{S}_i^B \cdot \vec{S}_{i+n}^B \rangle \right] / 2, \quad (15)$$

for  $n = 0, 2, 4, 6, \dots$

The average  $\langle \vec{S}_i^A \cdot \vec{S}_{i+n}^A \rangle$  in Equation (15) includes an average over sites  $\{i\}$  on which A chains are grafted, in order to improve the statistics. If perfect long range order occurs, as implied in Figure 4a, we clearly have  $C_n=1$  independent of  $n$ , while for the case of short range order, we expect  $C_n \propto \exp(-n/\xi)$ . Actually, considering the fact that we use a periodic boundary condition, i.e.  $C_n = C_{L_b-n}$ , we have analyzed our numerical data in terms

of the ansatz

$$C_n \propto \{ \exp(-n/\xi) + \exp[-(L_b - n)/\xi] \} \quad (16)$$

Figures 9 and 10 show our data for  $C_n$  for two choices of  $N$ : indeed we recognize that  $C_n$  decays to zero with increasing  $n$ , but the increase does get slower with increasing side chain length  $N$ . The scale of this correlation effect clearly increases with decreasing  $q_{AB}$ . While for  $N=6$  the correlation length  $\xi$  hardly depends on  $q_{AB}$ , for large  $N$  a slight increase of  $\xi$  with decreasing  $q_{AB}$  is suggested. In a poor solvent, the decay of  $C_n$  with  $n$  is much slower indicating a distinctly larger correlation length. This result gives a quantitative evidence for the

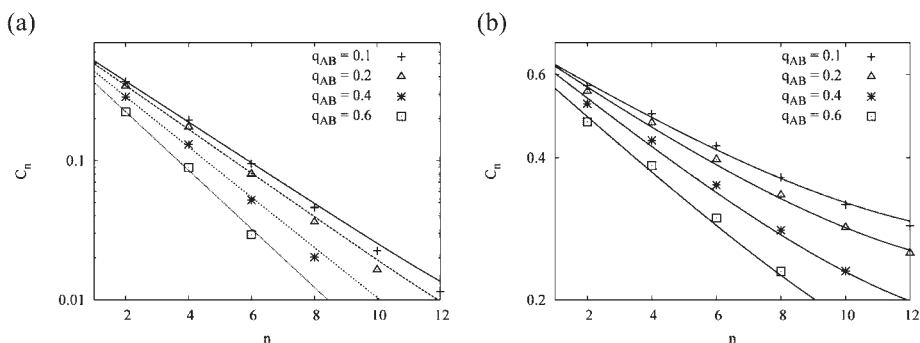


**Figure 10.**

Correlation function  $C_n$  plotted vs.  $n$  on a semi-log scale, for a poor solvent ( $q=1.5$ ),  $L_b=32$ , (a)  $N=6$  and (b)  $N=18$ . Several choices of  $q_{AB}$  are included, as indicated.

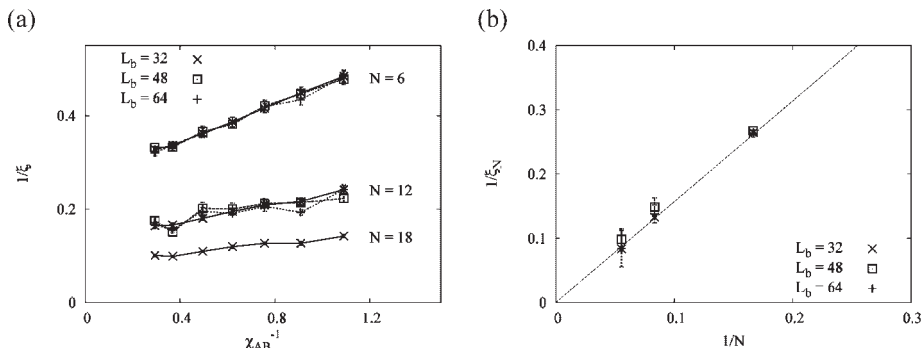


**Figure 11.**

(a) Inverse of correlation lengths  $\xi$  vs.  $\chi_{AB}^{-1}$  for copolymer bottle-brushes in a poor solvent ( $q=1.5$ ), with backbone length  $L_b=32, 48$ , and  $64$ , and three chain lengths  $N=6, 12$ , and  $18$ . (b) Inverse of the correlation length  $\xi_N$  in the limit of  $\chi_{AB} \rightarrow \infty$  vs.  $1/N$  for a poor solvent ( $q=1.5$ ). The straight line shows the asymptotic behavior as  $N \rightarrow \infty$ .

qualitative observation made already on the basis of the snapshot pictures, Figure 7b. Results for the correlation length  $\xi$ , determined by fitting  $C_n$  to Equation (16) in a poor solvent, are shown in Figure 11a.  $\xi$  increases gradually with increasing chemical incompatibility  $\chi_{AB}$  (decreasing temperature), and with increasing  $N$ . Since  $1/\xi$  decreases linearly as  $\chi_{AB}^{-1} \rightarrow 0$ , one can extrapolate the data to  $\chi_{AB}^{-1} = 0$  by fitting a straight line  $1/\xi = 1/\xi_N + b/\chi_{AB}$ . Results for  $\xi_N$  in a poor solvent are shown in Figure 11b. It gives an indication that a sharp phase transition only develops in the limit  $\chi_{AB}^{-1} \rightarrow 0$  and  $N \rightarrow \infty$ .

## Conclusion

In summary, we have studied bottle-brush polymers with a straight rigid backbone using the PERM algorithm. For one-component bottle-brush polymers in a good solvent, we verify the cross-over scaling prediction of the mean-square end-to-end distance in the radial direction. We also observe that there is a rather gradual and smooth crossover rather than a kink-like behavior of the scaling function. The full understanding of the structure of bottle-brush polymers in detail is still in process. For binary bottle-brush polymers we have presented the evidence that the phase

separation towards a “Janus cylinder” structure develops completely gradually as the incompatibility between the two types of monomers increases. In analogy to the one-dimensional XY model, long wavelength random “twist”-like rotation of the local interface between the A-rich and B-rich region in the “Janus cylinder” costs very little energy and destroys long range order completely. On the other hand, varying the chemical incompatibility and solvent quality, one can influence the occurrence of local phase separation and control the nanoscopic length scale over which Janus-type phase separation occurs along the backbone of the bottle brush.

**Acknowledgements:** This work was financially supported by the Deutsche Forschungsgemeinschaft (DFG) SFB 625/A3 and grant DFG-RUS 113/791/0. K. B. thanks S. Rathgeber and M. Schmidt for stimulating discussions. H.-P. H. thanks P. Grassberger and W. Nadler for very useful discussions.

- [1] A. Ciferri, W. Krigbaum, R. Meyer, “*Polymer Liquid Crystals*”, Academic Press, New York **1982**.
- [2] G. Wegner, *Mol. Cryst. Liq. Cryst. Sci. Technol. A* **1992**, 216, 7.
- [3] Y. Cao, P. Smith, *Polymer* **1993**, 34, 3139.
- [4] C. Li, N. Gunari, K. Fischer, A. Janshoff, M. Schmidt, *M. Angew. Chem. Int. Ed.* **2004**, 43, 1101.
- [5] T. M. Birshtein, E. B. Zhulina, *Polymer* **1984**, 25, 1453.

- [6] T. Witten, P. A. Pincus, *Macromolecules* **1986**, 19, 2509.
- [7] T. M. Birshtein, O. V. Borisov, Ye. B. Zhulina, A. R. Khokhlov, T. A. Yurasova, *Polym. Sci. USSR* **1987**, 29, 1293.
- [8] Z. Wang, S. A. Safran, *J. Chem. Phys.* **1988**, 89, 5323.
- [9] C. Ligoure, L. Leibler, *Macromolecules* **1990**, 23, 5044.
- [10] R. C. Ball, J. F. Marko, S. T. Milner, T. A. Witten, *Macromolecules* **1991**, 24, 693.
- [11] M. Murat, G. S. Grest, *Macromolecules* **1991**, 24, 704.
- [12] N. Dan, M. Tirell, *Macromolecules* **1992**, 25, 2890.
- [13] C. M. Wijmans, E. B. Zhulina, *Macromolecules* **1993**, 26, 7214.
- [14] H. Li, T. A. Witten, *Macromolecules* **1994**, 27, 449.
- [15] E. M. Sevick, *Macromolecules* **1996**, 29, 6952.
- [16] N. A. Denesyuk, *Phys. Rev. E* **2003**, 67, 051803.
- [17] M. Daoud, J. P. Cotton, *J. Phys. (Paris)* **1982**, 43, 531.
- [18] S. Alexander, *J. Phys. (Paris)* **1977**, 38, 953.
- [19] P. G. de Gennes, *Macromolecules* **1980**, 13, 1069.
- [20] A. Halperin, "Soft Order in Physical Systems", Y. Rabin, R. Bruinsma, Eds., Plenum Press, New York **1994**, p. 33.
- [21] P.-J. Flory, "Principles of Polymer Chemistry", Cornell University Press, Ithaca, New York **1953**.
- [22] P. G. de Gennes, "Scaling Concepts in Polymer Physics", Cornell University Press, Ithaca, New York **1979**.
- [23] S. Rathgeber, T. Pakula, A. Wilk, K. Matyjaszewski, K. L. Beers, *J. Chem. Phys.* **2005**, 122, 124904; S. Rathgeber, T. Pakula, A. Wilk, K. Matyjaszewski, H.-I. Lee, K. L. Beers, *Polymer* **2006**, 47, 7318.
- [24] B. Zhang, F. Gröhn, J. S. Pedersen, K. Fischer, M. Schmidt, *Macromolecules* **2006**, 39, 8440.
- [25] P. Grassberger, *Phys. Rev. E* **1997**, 56, 3682.
- [26] H.-P. Hsu, W. Nadler, P. Grassberger, *Macromolecules* **2004**, 37, 4658.
- [27] H.-P. Hsu, P. Grassberger, *Europhysics Lett.* **2004**, 66, 874.
- [28] T. Stephan, S. Muth, M. Schmidt, *Macromolecules* **2002**, 35, 9857.
- [29] R. Stepanyan, A. Subbotin, G. ten Brinke, *Macromolecules* **2002**, 35, 5640.
- [30] J. de Jong, G. ten Brinke, *Macromol. Theory Simul.* **2004**, 13, 318.
- [31] H.-P. Hsu, W. Paul, K. Binder, *Europhys. Lett.* **2006**, 76, 526.
- [32] G. S. Grest, M. Murat, "Monte Carlo and Molecular Dynamics Simulations in Polymer Science", K. Binder, Ed., Oxford University press, New York **1995**, p. 476.
- [33] C. Domb, M. S. Green, "Phase transitions and critical phenomena", Vol. 1, Academic press, New York **1971**.
- [34] R. J. Baxter, "Exactly solved models in statistical Mechanics", Academic Press, New York **1982**.
- [35] M. E. Fisher, V. Privman, *Phys. Rev. B* **1975**, 32, 477; J. L. Pichard, G. Sarma, *J. Phys. C* **1981**, 14, L617.